Available online at www.sciencedirect.com
ScienceDirect
Journal of Catalysis 245 (2007) 301–307
JOURNAL OF CATALYSIS
www.elsevier.com/locate/jcat

The role of SO_2 in the reduction of NO by CO on La_2O_2S

Ngai T. Lau *, Ming Fang, Chak K. Chan

Department of Chemical Engineering, The Hong Kong University of Science and Technology, Clear Water Bay, Hong Kong

Received 7 June 2006; revised 11 October 2006; accepted 23 October 2006

Available online 28 November 2006

Abstract

The decomposition of NO and the reduction of NO by CO on La_2O_2S were studied using temperature-programmed reaction technique coupled with fast mass spectrometry, powder X-ray diffraction and X-ray photoelectron spectroscopy. The role of SO_2 plays in the reduction is explored. It is found that the decomposition of NO is a favorable reaction step for the reduction of NO by CO achieved through a sulfur-assisted path. The oxygen produced in the decomposition is removed by the sulfur in the oxysulfide as SO_2, which in turn is reduced back to sulfur by CO on La_2O_2S. An external supply of sulfur, such as SO_2, in the feed is needed to maintain the population of sulfur in the oxysulfide and thus make the reduction sustainable.

Keywords: Lanthanum oxysulfide; Decomposition; Reaction step; Temperature-programmed reaction; XPS

1. Introduction

Lanthanum oxysulfide (La_2O_2S) has been shown to be highly active for the simultaneous reduction of SO_2 and NO by CO, but when SO_2 is absent, the reduction of NO cannot be sustained, and the conversion of NO drops significantly with time [1]. This suggests that the reduction of NO is closely coupled to the reduction of SO_2. However, the role that SO_2 plays in the reduction of NO remains unknown, and the reaction steps involved in the reduction of NO on La_2O_2S have not been studied and reported. In contrast, the reduction and decomposition of NO on La_2O_3 have been studied extensively [2–8] and can be used as a reference for the study of the oxysulfide reaction system. La_2O_3, the precursor of La_2O_2S [9], has a structure close to that of La_2O_2S, with one oxide ion replaced by a sulfide ion.

The reduction and decomposition of NO on La_2O_3 are usually associated with oxygen anion vacancies. In particular, Winter [2] proposed that the decomposition of NO starts with the adsorption of NO molecules at R2 centers. An R2 center is basically a pair of adjacent oxygen anion vacancies; the oxygen remaining from the NO occupies the center after decomposition. The study of the adsorption and decomposition of NO on La_2O_3 by Huang et al. [7] supports the R2 center decomposition mechanism. It is interesting to note that when NO is fed to La_2O_3 that has been heated in helium at 973 K and cooled to room temperature, a small amount of N_2O is produced. This indicates that decomposition of NO will readily occur even at room temperature if anion vacancies are made available:

$$2NO \rightarrow N_2O + O. \quad (1)$$

On La_2O_2S, oxygen anion vacancies are probably formed in a manner comparable to that on the oxide, and also can be produced via the sulfur pathway, as reported by Lau and Fang [10]:

$$^*S \rightarrow S + ^*, \quad (2)$$

where $^*S$ is a sulfide ion in the surface lattice and * is an anion vacancy with a negative charge. Thus, it is fair to suggest that NO is also readily decomposed on La_2O_2S provided that these anion vacancies are available. Winter [11] pointed out that in the decomposition of NO, the desorption of oxygen to regenerate the vacancies can be the limiting step. Thus, if we can identify a chemical species in La_2O_2S that promotes the removal of oxygen and regenerates the anion vacancies at temperatures typical of NO reduction, then the proposition that the decomposition of NO is an important step in the reduction of NO on La_2O_2S can be substantiated. The goal of this paper is to identify the species in the oxysulfide that can remove the

* Corresponding author. Fax: +852 2719 6710.
E-mail address: ntlau@ust.hk (N.T. Lau).

0021-9517/$ – see front matter
doi:10.1016/j.jcat.2006.10.025

oxygen at the typical reaction temperatures, and by doing so demonstrate that the decomposition of NO is an important reaction step for the reduction of NO by CO on La_2O_2S.

In this study, we used temperature-programmed reaction coupled with fast mass spectrometry (TPR/MS) to track the decomposition and the reduction of NO in the presence and absence of SO_2 by CO on La_2O_2S with reference to those on La_2O_3. Changes in the catalyst composition due to the NO reactions were monitored with powder X-ray diffraction (XRD) and X-ray photoelectron spectroscopy (XPS). The TPR/MS technique temporally and thermally isolates the interactions between the reactants and the catalyst and allows identification of the active species in the catalyst.

2. Experimental

2.1. Catalyst preparation

La_2O_2S was synthesized in situ in a quartz microreactor following the sulfidization procedure reported by Ma et al. [9] from $La(OH)_3$ powder (Yiaolong, China) at 700 °C for 3 h. The sample was kept in flowing Ar or He before use. The composition of the sample material synthesized was La_2O_2S, as confirmed by XRD, and the sample's specific surface area was approximately 4 $m^2\,g^{-1}$ as obtained with the BET method (ASAP2000, Micromeritics).

La_2O_3 was also prepared in situ in a quartz microreactor by calcining the $La(OH)_3$ powder at 700 °C for 3 h in flowing Ar at ∼90 ml min^{-1}. The composition of the sample was La_2O_3, as confirmed by XRD, and the sample's specific surface area was approximately 4 $m^2\,g^{-1}$, as obtained with BET.

2.2. TPR/MS

TPR/MS measurements were obtained using the experimental setup shown in Fig. 1. A 0.1-g sample of La_2O_2S was used in each measurement. The feed gas, at 100 ml min^{-1}, 25 °C, and 1 atm, with typical composition

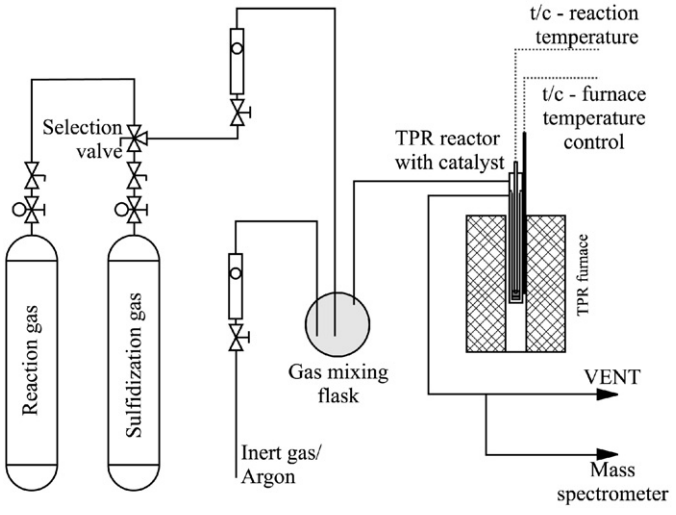

Fig. 1. Flow schematic of experiment setup.

(C1) 0.04%v NO,
(C2) 0.4%v SO_2, 0.8%v CO,
(C3) 0.16%v NO, 0.16%v CO, and
(C4) 0.16%v NO, 0.4%v SO_2, 0.96%v CO,

was obtained by diluting the preblended reaction gases with Ar in the gas-mixing flask before it was fed to the reactor. The composition of the effluent gas from the reactor was continuously monitored with the mass spectrometer (Extrel MS250), which reported the composition data each second.

The typical TPR procedure started with purging the sample with feed gas at room temperature (∼25 °C) until the composition of the effluent from the reactor was steady. The sample was then heated from room temperature to 700 °C at 10 °C min^{-1} and kept at 700 °C for 2 h or until the composition of the effluent gas was steady.

2.3. Catalyst composition

The bulk composition of the catalyst was monitored with XRD using a Philips model PW1830 powder X-ray diffraction system equipped with a Cu anode and a graphite monochromator operated at 2 kW. The samples were spread and pressed onto glass sample holders with no pretreatment.

The surface composition of the catalyst was measured by XPS (Perkin–Elmer Surface Science Analysis System model PHI 5600) equipped with a monochromatic Al$K\alpha$ X-ray source according to the procedure described by Lau and Fang [10]. The powder samples were pressed into cup-shaped sample mounts for direct insertion into the instrument. Low-energy flooding electrons were used to neutralize the charges built up on the samples, and the binding energy (BE) scale was so adjusted to make the adventitious carbon peak at 284.5 eV. Multiplex scans of carbon C1s, nitrogen N1s, oxygen O1s, sulfur S2p, and lanthanum La3d were acquired at constant pass energy of 23.5 eV.

3. Results

3.1. Change in catalyst composition

The XPS C1s, O1s, S2p, and La3d spectra of La_2O_2S used in the decomposition and reduction of NO in the presence and absence of SO_2 are shown in Fig. 2. The as-sulfidized sample is also presented as a reference. The typical O1s and S2p peaks are listed in Table 1. The as-sulfidized sample XPS spectra are comparable to those reported by Lau and Fang [10]. Although most of the samples were subjected to the reactions involving NO, no detectable amount of nitrogen was found on their surfaces. The C1s spectrum contained two peaks: a higher-intensity peak at 284.5 eV, attributable to adventitious carbon, and a lower-intensity peak at ∼289 eV, associated with C–O species, such as carbonate. S2p at BE ∼160.1 eV can be assigned to the sulfide in the lattice or the sulfur in the surface not bonded to oxygen. The broader group of S2p at ∼166.4–168.5 eV can be attributed to S–O species, such as SO_2 adspecies, sulfite, and sulfate. O1s also contained two peaks, one at lower BE

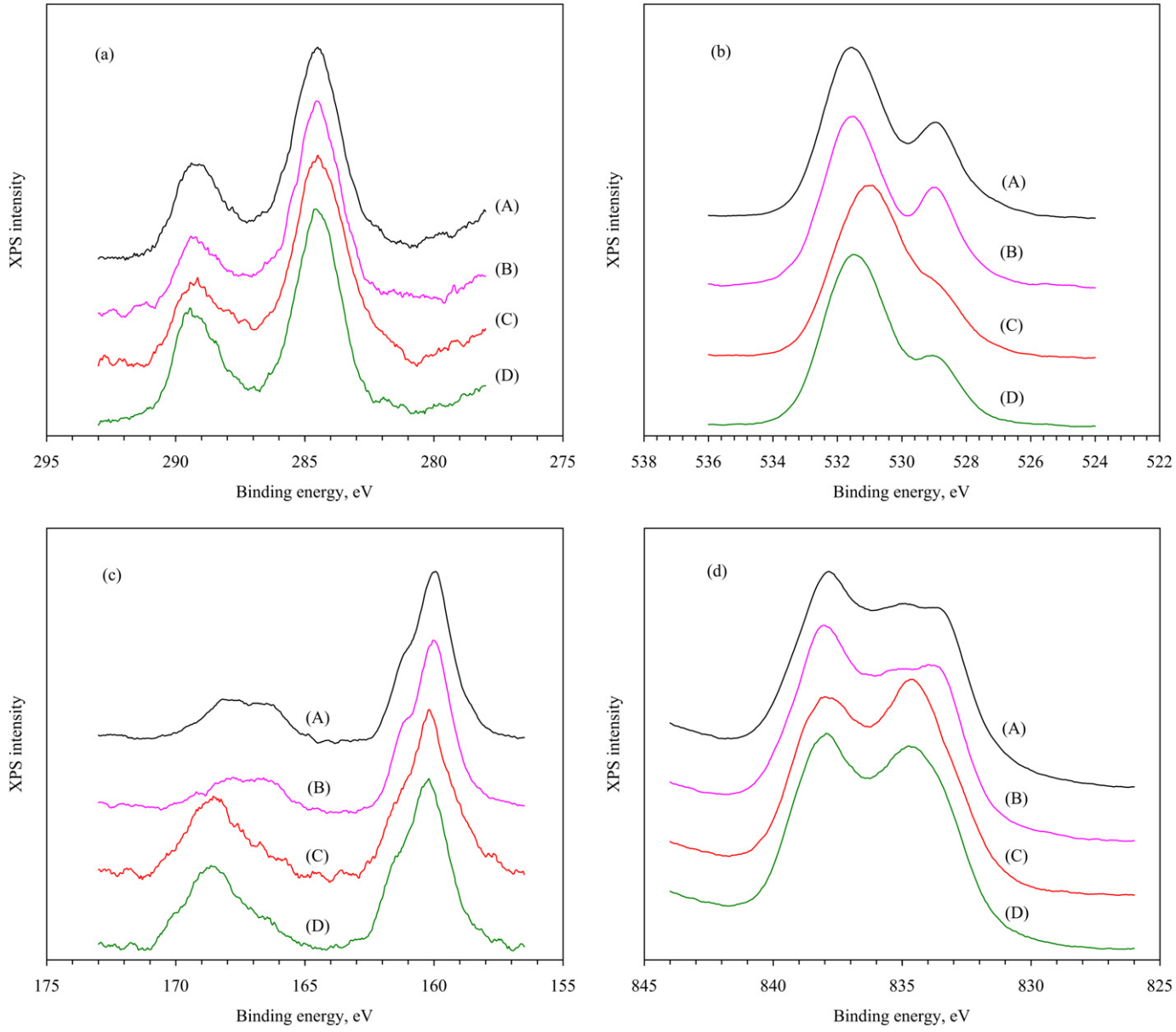

Fig. 2. XPS spectra (a) C1s, (b) O1s, (c) S2p and (d) La3d$_{5/2}$ of La_2O_2S—effect of NO. Curves in the figures from top to bottom, (A) no treatment (as-sulfidized), (B) TPR reaction with NO, SO_2 and CO, (C) TPR reaction with NO and CO, and (D) TPR reaction with NO. All the spectra have been rescaled to the same vertical span.

Table 1
Effect of NO reactions on XPS O1s and S2p peaks of La_2O_2S

Reactions	Binding energy (eV)			
	O1s		S2p	
As-sulfidized	531.6	528.9	160.0	166.4–168.0
NO decomposition	531.5	528.9	160.2	168.5
NO reduction by CO	530.9	–	160.2	168.3
NO reduction by CO in the presence of SO_2	531.5	528.9	160.1	166.4–167.7

The oxysulfide was produced by sulfidizing lanthanum hydroxide powder with a stoichiometric mixture of SO_2 and CO.

(∼528.9 eV) due to lattice oxygen or oxygen not related to C–O or S–O species, and the other at higher BE comprising contributions from the C–O and S–O species.

XRD revealed no significant changes in the bulk composition of the La_2O_2S catalyst after the NO reactions, although XPS revealed subtle changes in the surface composition. Table 2 shows the changes in the carbon, oxygen, and sulfur species in the surface of the catalyst due to the NO reactions. The decomposition of NO significantly decreased the concentration of sulfur in the surface relative to lanthanum (S/La), especially the sulfur not associated with the oxygen (S_{ONLY}/La), while increasing the concentrations of oxygen (O/La) and S–O species in the surface. Similar changes were also observed on La_2O_2S subjected to the reduction of NO by CO. The lattice oxygen O1s was almost completely diminished, and the O1s at higher BE shifted to 530.9 eV, indicating a dominant contribution from the carbonate [12]. The reduction of NO in the pres-

Table 2
Effect of NO reactions on the surface concentration of carbon, oxygen and sulfur in La_2O_2S

Reactions	C/La	O/La	S/La	S_{ONLY}/La	S–O/La	S–O/S
As-sulfidized	1.3	3.2	0.65	0.46	0.20	0.30
NO decomposition	1.9	4.0	0.55	0.32	0.23	0.41
NO reduction by CO	1.5	4.1	0.40	0.24	0.16	0.40
NO reduction by CO in the presence of SO_2	1.2	3.2	0.52	0.40	0.12	0.23

C/La, O/La and S/La are the relative atomic concentration of carbon, oxygen and sulfur to lanthanum obtained with the XPS measurements. S_{ONLY} is the sulfur species in the surface that is not bonded to oxygen such as sulfide. S–O/S is the relative atomic concentration of surface S–O species to the total sulfur species S.

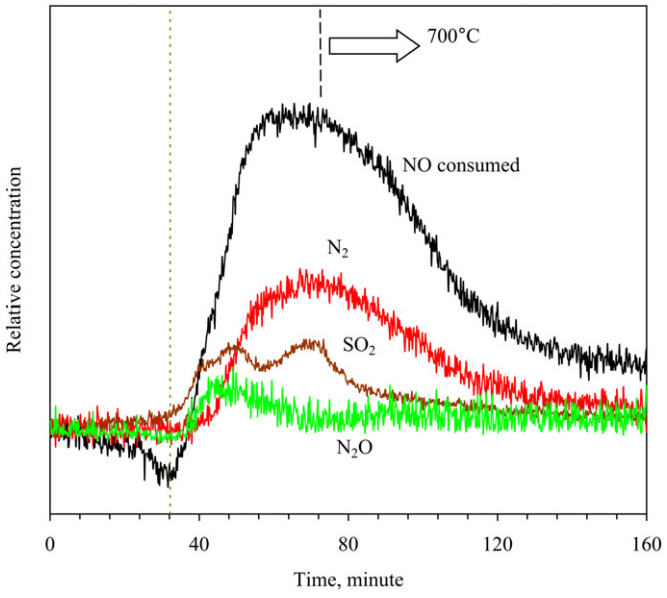

Fig. 3. Decomposition of NO on La_2O_2S. The nominal feed composition was 0.04%v NO. The relative concentrations of the species were obtained by correcting the intensity of $m/z = 28$, 30, 44 and 64 for zeroes and fragmentation effect, and then adjusting for the sensitivity of the compounds. The dashed line marks the beginning of the 700 °C reaction temperature zone. The dotted line marks the maximum NO desorption point.

ence of SO_2 reduced the concentrations of the sulfur and S–O species in the surface but did not change the surface oxygen concentrations. Thus, the decomposition and reduction of NO in the absence of SO_2 consumed surface sulfur and produced S–O species, whereas the reduction by CO kept the concentration of S–O species low. In the presence of SO_2, the sulfur consumed during NO reduction likely was replenished by the sulfur produced during SO_2 reduction.

3.2. Decomposition of NO: TPR/MS results

In Fig. 3, the temporal TPR/MS profile of the decomposition of NO on La_2O_2S shows that N_2 and N_2O were produced as NO was consumed. This indicates the following decomposition reactions:

$$2NO \rightarrow N_2 + 2O \quad (3)$$

and

$$2NO \rightarrow N_2O + O. \quad (1)$$

Instead of oxygen, SO_2 was produced; its formation was closely associated with the decomposition of NO. As NO decomposition diminished with time, SO_2 formation also slowed. SO_2 started to form at ~320, ~40 °C below the temperature at which significant amounts of N_2 and N_2O are formed. Furthermore, the SO_2 formation curve consisted of two temperature peaks. Based on the formation of COS by the reaction between CO and sulfur in La_2O_2S [10], the lower peak can be attributed to the reaction with labile sulfur in the surface, whereas the higher peak may be associated with the reaction with the lattice sulfur. Note that a significant amount of NO was desorbed immediately before the start of decomposition.

3.3. Reduction of NO: TPR/MS

Fig. 4 shows the thermal TPR/MS profile for the reduction of NO in the presence of SO_2. The conversion, C, is computed from the mass intensities using the following equation:

$$C = \frac{I_0 - I}{I_0}, \quad (4)$$

where I and I_0 are the net intensities of the selected mass fragment of the reactant species in the effluent and feed streams, respectively. For example, C_CO, the CO conversion, is computed from the intensities of fragment with mass-to-charge ratio $m/z = 28$ in effluent and feed. This intensity usually measures the CO concentration when CO is involved in the reaction. However, the formation of N_2 in the reduction of NO apparently lowers the conversion of CO due to the interference of N_2. The mass fragment also includes the contribution from CO_2 and N_2O, but their contribution is usually negligible relative to CO and N_2. Similarly, C_NO and C_SO_2, the conversions of NO and SO_2, are computed from intensities $m/z = 30$ and 64, respectively. C_NO also contains the fragment contribution from N_2O, but this usually is very small. C_SO_2 is usually not affected by other species except S_2 vapor. S_2 vapor is not volatile and is usually deposited on the cool surface of the reactor and transfer line; only a negligible fraction can enter into the mass spectrometer. The CO_2 intensity ($m/z = 44$) measures the concentration of the products of CO_2 but also may include contributions from N_2O. When there is significant conversion of CO, CO_2 will be the dominating species; however, when CO conversion is low, N_2O can be the dominant species.

In the presence of SO_2, the reduction of NO by CO began readily on La_2O_2S at ~440 °C, and high and sustained conversions of NO, CO, and SO_2 were attained at >500 °C. The reduction was almost impossible on La_2O_3; only very low conversions of NO, SO_2, and CO were detectable at >600 °C. This is consistent with the findings of Lau et al. [13] that anhydrous La_2O_3 could not be sulfidized to La_2O_2S and is inactive for the reduction of SO_2 by CO.

When SO_2 was absent (Fig. 5), the reduction of NO on La_2O_2S could not be sustained. Although a significant amount

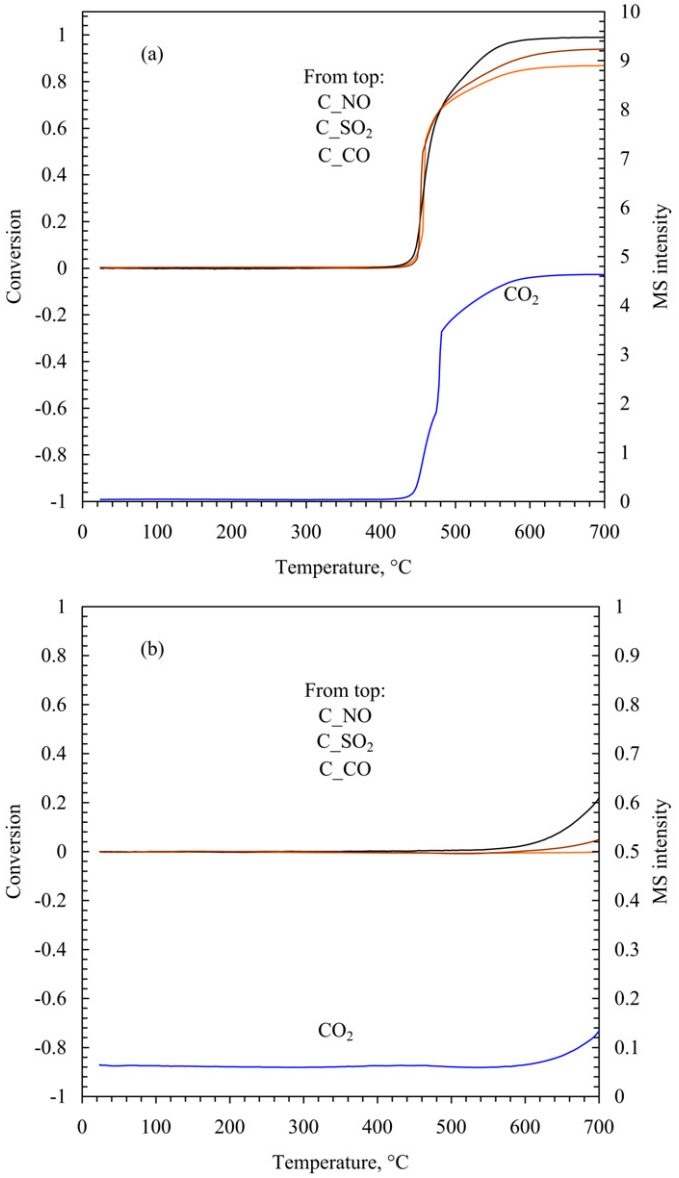

Fig. 4. Catalytic reduction of NO by CO on (a) La_2O_2S and (b) La_2O_3 in the presence of SO_2 ($NO/SO_2 = 0.4$). The C_CO, C_NO, and C_SO_2 are the conversion curves for CO, NO, and SO_2 obtained with the mass intensities $m/z = 28$, 30 and 64, respectively, and use the left scale. The scale of the CO_2 ($m/z = 44$) intensity curve is on the right.

of NO was reduced with the formation of SO_2, CO_2, and possibly N_2O in the first TPR program at >320 °C, a negligible amount of NO and CO reacted in the second TPR, with no SO_2 formed. The conversion of CO in the first TPR was significantly lower than that of NO, probably due to the interference of N_2 to C_CO and the fact that NO decomposition was the dominant reaction. Almost no reduction was observed on La_2O_3.

In summary, the reduction of NO by CO did not occur on La_2O_3 irrespective of the presence or absence of SO_2; however, on La_2O_2S, the reduction was sustained with high conversion of NO, CO, and SO_2 in the presence of SO_2. In the absence of SO_2, the NO reaction also could not be sustained, and it eventually died out when the formation of SO_2 ceased.

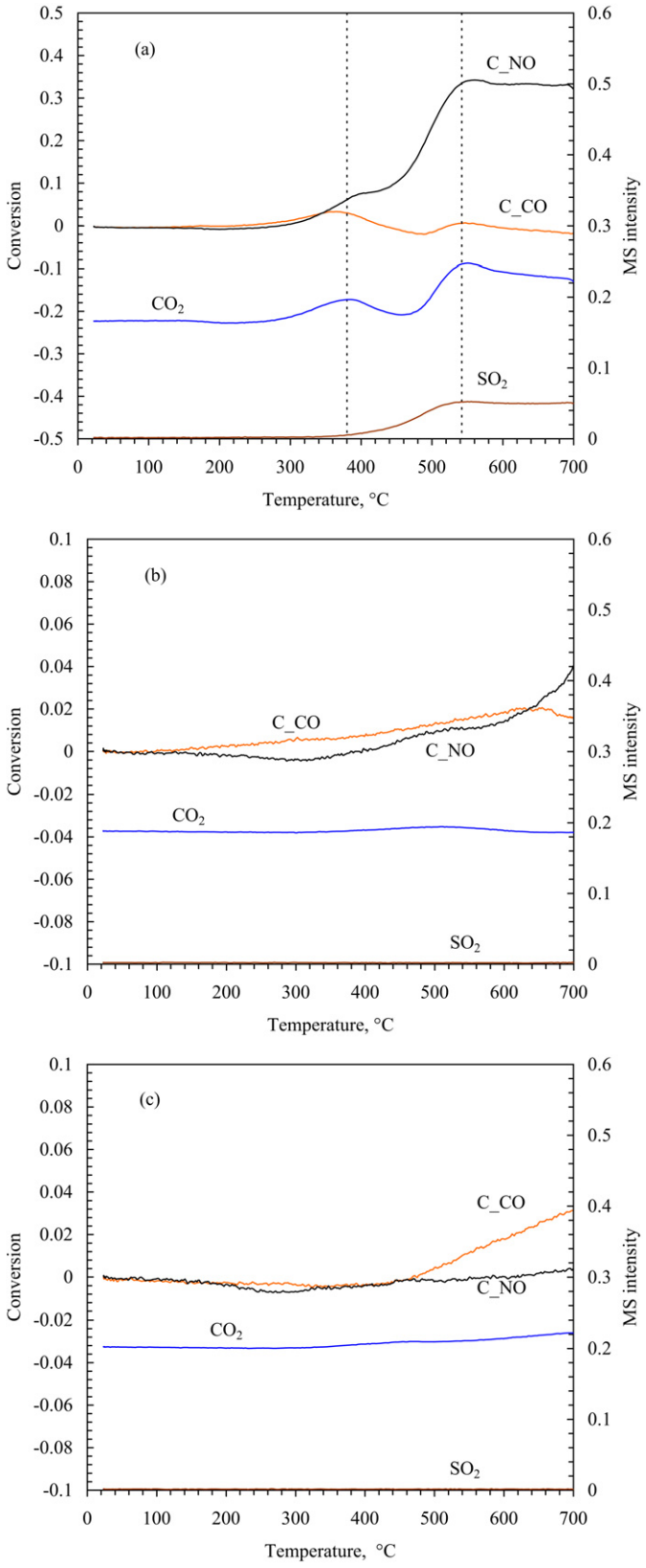

Fig. 5. Catalytic reduction of NO by CO on (a–b) La_2O_2S and (c) La_2O_3 in the absence of SO_2; (a) is the result of the first temperature program. The C_CO and C_NO are the CO and NO conversion curves obtained with the mass intensities $m/z = 28$ and 30, respectively, and use the left scale. The scale of the CO_2 ($m/z = 44$) and SO_2 ($m/z = 64$) intensity curves is on the right. The dotted lines mark the two CO_2 bumps in (a).

4. Discussion

The TPR/MS and XPS results both show that the decomposition and reduction of NO are closely associated with the sulfur in the catalyst and the oxidation of the sulfur to SO_2. This was also observed in the reduction of NO on supported sulfides on γ-Al_2O_3 [14], CoS_X–TiO_2 [15], and Ti–Sn solid solution catalysts [16]. The sulfur produced in the reduction of SO_2 helps remove the oxygen from the decomposition of NO as SO_2, that is, the sulfur-assisted reduction of NO. It is possible that the reduction of NO on La_2O_2S also follows a similar pathway:

$$S + 2O \rightarrow SO_2. \quad (5)$$

Removing the oxygen helps regenerate the anion vacancies for the next NO decomposition cycle.

Taking SO_2 formation as an indicator for the decomposition of NO, the NO decomposition ignition temperature (Fig. 3) will be ∼320 °C. This is approximately the same temperature at which a significant amount of NO was reacted in the reduction of NO on La_2O_2S in the absence of SO_2. This temperature was also ∼100 °C lower than the temperature at which significant NO reduction was observed in the presence of SO_2. Thus, the decomposition of NO is a favored reaction between NO and La_2O_2S.

As sulfur is consumed to remove the oxygen and regenerate the anion vacancies, the available sulfur in the oxysulfide is eventually used up if not replenished. Presumably, the SO_2 produced in the decomposition of NO can be reduced to replenish the oxysulfide. But insufficient sulfur is available for this, because a portion of the sulfur species is lost to the effluent stream. An additional supply of sulfur, such as the SO_2 in the feed, is needed. This is why the reduction of NO can be sustained only in the presence of SO_2 in the feed.

The reduction of NO by COS is probably one of the competing reaction paths for the reduction of NO over La_2O_2S, especially when COS is present in the feed. Ma et al. [1] reported that the reduction of NO by COS can be significant at temperatures as low as 150 °C over La_2O_2S. However, if COS is absent from the feed and must be produced by the reaction between the sulfur in the oxysulfide and CO [10], then the COS reaction path probably will not be as effective as the reaction path via NO decomposition. This is because the NO decomposition path is a more direct reaction path involving the sulfur, whereas the COS path is an indirect path in which COS must be formed at temperatures above 340 °C [10] and there is serious competition for COS from the reduction of SO_2 [18].

Fig. 3 indicates that SO_2 was produced before the NO decomposition reaction. Some of the SO_2 could be the residual adspecies from the sulfidization process when we synthesized the oxysulfide, whereas the remainder could be formed by the oxidation of sulfur by the oxygen produced in the decomposition of the adsorbed NO on the oxysulfide. A significant amount of NO was desorbed from the oxysulfide when SO_2 started to form, as shown in Fig. 3. The desorption created vacant adsorption sites. This suggests that additional vacant sites promoted the decomposition of NO. Furthermore, nitrogen products (N_2 and N_2O) were formed well after SO_2 was produced, indicating that nitrogen was held more tightly by the oxysulfide, probably at the anion vacancies (the adsorption sites). This suggests that the NO is adsorbed on La_2O_2S with the N-end at the vacancies differing from Winter's decomposition scheme with the O-end at the vacancies [2]. The DRIFTS study on the decomposition of NO on La_2O_3 by Huang et al. [7] also reported NO adspecies with the N-end at the oxysulfide. In addition, nitrogen, being less electronegative than oxygen, can be slightly more positively charged, making the N-ends more readily approach the negatively charged anion vacancies. There is also another possibility that the decomposition of NO on La_2O_2S can be accomplished with two adjacent anion vacancies,

$$NO + 2^* \rightarrow {}^*N + {}^*O, \quad (6)$$

where * represents an anion vacancy. However, further research is needed to clarify this issue.

Furthermore, N_2O is the preferential product for the decomposition of NO at low temperatures when the reaction started (see Fig. 3). As more NO is consumed at higher temperatures, N_2 becomes the dominant product. This shift in N_2 selectivity may be associated with the population of N resulting from NO decomposition. When plenty of N is produced at sufficiently high temperature, N_2 is readily and preferentially formed by the combination of N. At low temperatures, where N is relatively scarce, there is greater likelihood of N reacting with another NO to form N_2O before N_2 formation can occur.

Therefore, it is likely that the reduction of NO on La_2O_2S follows these reaction steps:

Step 1: Adsorption of NO at the adsorption sites.
Step 2: Decomposition of NO to N and O.
Step 3: Removal of O by the oxidation of sulfur in La_2O_2S to SO_2.
Step 4: Desorption of nitrogen as N_2.
Step 5: Reduction of SO_2 by CO to sulfur.

The adsorption sites are the anion vacancies in the surface of La_2O_2S. Step 5 maintains the sulfur population in the oxysulfide and guarantees that sufficient sulfur is available to remove O in Step 3.

The role of SO_2 in NO reduction is schematically illustrated in Fig. 6. This diagram also explains how NO reduction is linked to the reduction of SO_2 on La_2O_2S. The lower reaction cycle shows the COS-intermediate mechanism for the reduction of SO_2 by CO on La_2O_2S [10,17,18]. The COS intermediate is formed when CO reacts with sulfur in the oxysulfide. The intermediate then reacts with SO_2 on the La_2O_2S to produce sulfur and CO_2. The NO reaction cycle is represented by the upper cycle. Sulfur in the oxysulfide fuels the decomposition of NO to N_2 by forming SO_2, which is in turn reduced by CO to sulfur in the SO_2 reduction cycle. Thus, the S–SO_2 pair facilitates the NO reaction—an indirect reduction path of NO by CO.

5. Conclusion

This study of the decomposition of NO and the reduction of NO by CO in the presence and absence of SO_2 on La_2O_2S

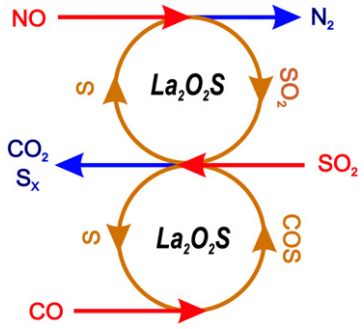

Fig. 6. Coupling between the reduction of NO and the reduction of SO_2 on La_2O_2S—an illustration.

found that the decomposition reaction is the favored reaction step in the reduction of NO by CO and that the reduction proceeds via the sulfur-assisted path. The oxygen produced in the decomposition is removed by sulfur in the oxysulfide as SO_2, which is then reduced back to sulfur by CO on La_2O_2S. This step helps regenerate the anion vacancies for NO decomposition. The S–SO_2 pair facilitates the indirect reduction of NO by CO to nitrogen through the SO_2 reduction cycle. An external supply of sulfur, such as SO_2 in the feed, must be available to sustain the NO reduction process.

Acknowledgments

This work was supported by the Research Grant Council of the Hong Kong Special Administration Region, China (Project HKUST6001/01P). The authors thank Professor J.X. Ma of Tongji University, Shanghai, China, for his helpful advice and comments.

References

[1] J.X. Ma, M. Fang, N.T. Lau, Catal. Lett. 62 (1999) 127.
[2] E.R.S. Winter, J. Catal. 22 (1971) 158.
[3] X. Zhang, A.B. Walters, M.A. Vannice, Appl. Catal. B 4 (1994) 237.
[4] X.X. Zhang, A.B. Walters, M.A. Vannice, NO reduction by CH_4 over rare earth oxides, in: G. Centi, C. Cristiani, P. Forzatti, S. Perathoner (Eds.), Environmental Catalysis—For a Better World and Life: Proc. 1st World Conference, Pisa, 1–5 May 1995, SCI Publisher, Rome, 1995, p. 33.
[5] M.A. Vannice, A.B. Walters, X. Zhang, J. Catal. 159 (1996) 119.
[6] S.J. Huang, A.B. Walters, M.A. Vannice, J. Catal. 173 (1998) 229.
[7] S.J. Huang, A.B. Walters, M.A. Vannice, J. Catal. 192 (2000) 29.
[8] T.J. Toops, A.B. Walters, M.A. Vannice, Appl. Catal. B 38 (2002) 183.
[9] J.X. Ma, M. Fang, N.T. Lau, J. Catal. 163 (1996) 271.
[10] N.T. Lau, M. Fang, J. Catal. 179 (1998) 343.
[11] E.R.S. Winter, J. Catal. 34 (1974) 440.
[12] J.F. Moulder, W.F. Stickle, P.E. Sobol, K.D. Bomben, in: J. Chastain (Ed.), Handbook of X-ray Photoelectron Spectroscopy—A Reference Book of Standard Spectra for Identification and Interpretation of XPS Data, Physical Electronic Division, Perkin–Elmer Corporation, Eden Prairie, MN, 1992.
[13] N.T. Lau, M. Fang, J.X. Ma, Appl. Catal. B 26 (2000) 81.
[14] S. Zhuang, M. Yamazaki, K. Omata, Y. Takahashi, M. Yamada, Appl. Catal. B 31 (2001) 133.
[15] Z. Zhang, J. Ma, X. Yang, J. Mol. Catal. A Chem. 195 (2003) 189.
[16] Z. Zhang, J. Ma, X. Yang, Chem. Eng. J. 95 (2003) 15.
[17] J.X. Ma, M. Fang, N.T. Lau, Appl. Catal. A 150 (1997) 253.
[18] N.T. Lau, M. Fang, C.K. Chan, J. Mol. Catal. A Chem. 203 (2003) 221.